
Article:
Jana, Kamalesh, Lad, Amit D., West, David et al. (6 more authors) (2021) Femtosecond, two-dimensional spatial Doppler mapping of ultraintense laser-solid target interaction. Physical Review Research. 033034. ISSN 2643-1564

https://doi.org/10.1103/PhysRevResearch.3.033034

Femtosecond, two-dimensional spatial Doppler mapping of ultraintense laser-solid target interaction

Kamalesh Jana [1,*] Amit D. Lad [1] David West [2] Will Trickey [2] Chris Underwood [2]
Yash M. Ved,[1] A. P. L. Robinson,[3] J. Pasley [2] and G. Ravindra Kumar [1,†]

[1] *Tata Institute of Fundamental Research, Dr. Homi Bhabha Road, Colaba, Mumbai 400005, India*
[2] *York Plasma Institute, Department of Physics, University of York, Heslington, York YO10 5DD, United Kingdom*
[3] *Central Laser Facility, STFC Rutherford Appleton Laboratory, Harwell Campus, Didcot OX11 0QX, United Kingdom*

(Received 27 October 2020; accepted 11 May 2021; published 9 July 2021)

We present measurements of the spatiotemporal evolution of a hot-dense plasma generated by the interaction of an intense 25 fs laser pulse with a solid target, using pump-probe two-dimensional (2D) Doppler spectrometry. Measuring the time-dependent Doppler shifts at different positions across the probe beam, we achieve velocity mapping at hundreds of femtoseconds time resolution *simultaneously* with a few micrometer spatial resolution across the transverse length of the plasma. Simulations of the interaction using a combination of 2D particle-in-cell and 2D radiation hydrodynamics codes agree well with the experiment.

DOI: 10.1103/PhysRevResearch.3.033034

Ultraintense, femtosecond laser irradiation of a solid produces a dense, hot plasma that has emerged as a test bed for a wide range of phenomena ranging from basic plasma physics through to complex laser-plasma interactions and table-top approximations to astrophysical systems [1–3]. In addition, it offers myriad opportunities for scientific and technological development enabled by the ultrashort high-flux pulses of photons [4,5], charged particles [6–8], and neutral atoms [9] so produced. The hydrodynamics induced by a high-intensity short-pulse laser when it interacts with a solid target evolves on subpicosecond timescales. Resolving this dynamics, and obtaining a satisfactory, experimentally based, understanding of the physics requires diagnostic approaches that can resolve both the relevant length scales and timescales simultaneously.

In recent years, efforts have been made by ourselves and others to get to grips with the evolution of these plasmas on picosecond and sometimes subpicosecond timescales [10–20]. New phenomena such as terahertz acoustics [16] have been discovered and both shock wave generation [10–14] and control [14] have been investigated. All these efforts, however, lacked the ability to spatially resolve the dynamics in the transverse direction.

It is well known that the transverse evolution of the plasma is a crucial feature in intense laser-matter interactions. Long ago, critical surface rippling was postulated to account for resonance absorption at normal incidence [21]. More recent simulations have shown that the critical surface gets deformed by light pressure [22–24] and this leads to additional laser absorption.

Spatial imaging and two-dimensional (2D) reflectivity measurements of the plasma surface have shown interesting lateral transport of fast electrons and heat. The former has been shown to spread at speeds that are a significant fraction of the speed of light and cause rapid ionization and heating, away from the irradiated spot [25–27]. In interesting earlier studies, Borghesi *et al.* [28] and Palmer *et al.* [29], have used proton deflectometry to image the temporal evolution of instabilities and thermal transport on picosecond timescales and in one spatial dimension with high-energy, high-peak power lasers. Heat transport across the transverse dimension is an important issue as it depletes the amount of energy that can be coupled into the target. Simulations done much earlier have pointed to differences between 1D and 2D transport across the plasma length as well as Spitzer and non-Spitzer transport in the plasma [30]. The transverse evolution of velocity profiles could also be important for understanding plasma instabilities [31,32].

In this paper, we present an advance in the measurement of the ultrafast dynamics of the plasma, which enables spatial resolution in the transverse direction. Specifically, we obtain spatially resolved velocity maps of the plasma on subpicosecond and picosecond timescales with a few micrometer spatial resolution. Our technique thus enables, in combination with simulations, the mapping of the energy flow within the target driven by electron conduction and radiation transport on timescales that are relevant to the laser-plasma interaction and consequent heating. The lowest velocity that can be measured is of the order of 10^6 cm/s, enabling the diagnosis of plasmas with temperatures as low as 6 eV for carbon and even less for lower mass elements. Given that high-intensity laser-plasma interactions typically produce very much higher temperatures than this, the present diagnostic can be employed to examine transport and cooling across broad regions of the target. This diagnostic also enables the measurement of shock propagation

*kamaleshjana92@gmail.com
†grk@tifr.res.in

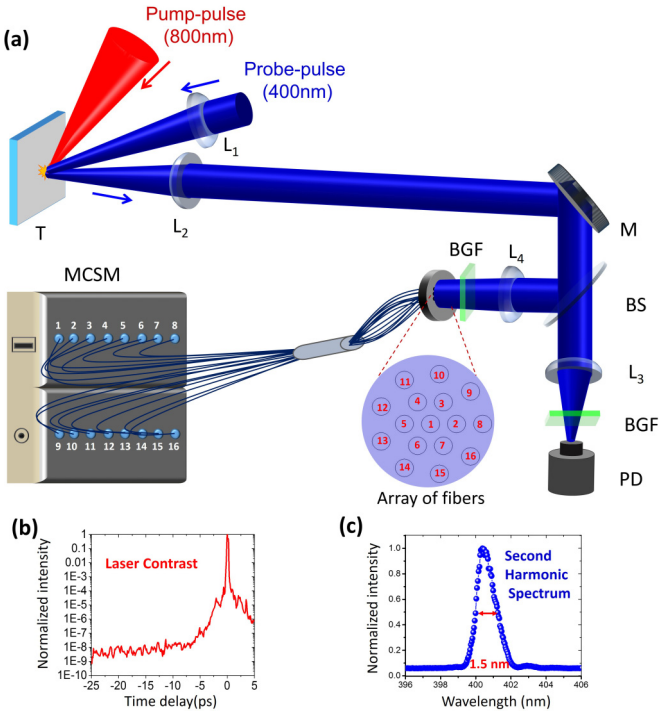

FIG. 1. (a) Schematic of experimental setup for 2D Doppler spectrometry. T: target (Al-coated BK-7 glass). M: mirror. L_1–L_4: lenses. BS: beam splitter. PD: photodiode. MCSM: multichannel high-resolution spectrometer connected with optical fibers. BGF: blue-green (BG-39) filter. (b) Laser intensity contrast measured by a third-order cross-correlator (SEQUOIA). (c) Spectrum of second harmonic probe pulse.

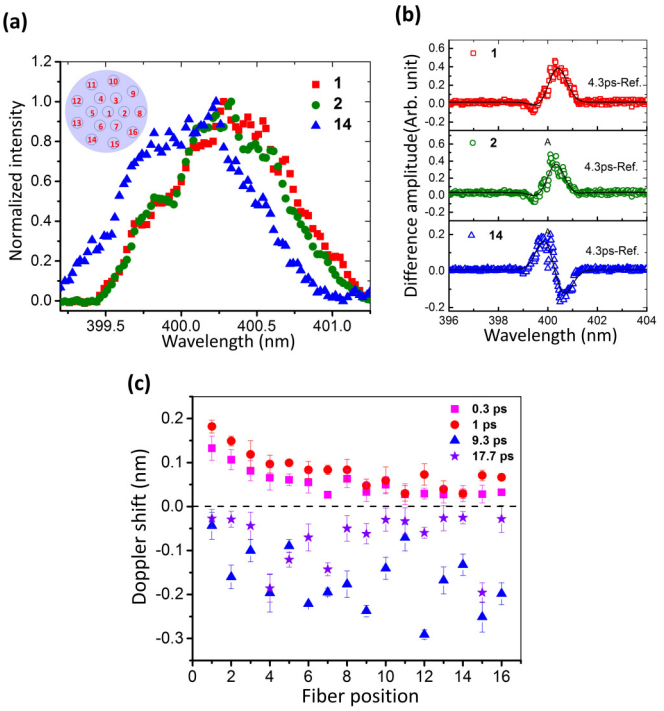

FIG. 2. (a) Normalized spectra of reflected probe measured at three different positions across the probe for a 4.3 ps time delay. The inset (top left) shows marked fiber positions across the probe. (b) Difference amplitudes (derived by subtracting the reference spectrum from the time-delayed spectra) at three different positions across the probe for 4.3 ps time delay. (c) Doppler shifts at different locations across the probe for four different time delays.

and curvature in thin targets, such as those typically employed in ion acceleration experiments. It is well known that shocks propagating through such targets can distort the rear surface, thus affecting the proton and ion beam divergence [33], making it crucial to know the two-dimensional shape of the plasma surface and hence the transverse variation of the electric field. Obtaining a better understanding of lateral energy transport is also crucial in a range of different problems, for example, in laser-generated particle and photon sources the size of the source can be a strong function of the degree of lateral transport. The present study with 16 spectrometers is aimed at demonstrating the principle and the capabilities of the method. With better imaging, an increased number of spectrometers, shorter or temporally shaped pulses, and different configurations of fibers, the spatial and temporal resolution can be enhanced. These improvements may also enable studies of transverse thermal transport and instabilities at the required resolution.

The experiment [Fig. 1(a)] was carried out at the Tata Institute of Fundamental Research (TIFR), Mumbai using a chirped pulse amplification based Ti:sapphire 100-TW laser system which can deliver 800-nm, 25-fs pulses with a repetition rate of up to 10 Hz. The intensity contrast [measured by a third-order cross-correlator (SEQUOIA)] of the laser pulse at 25 ps was $\sim 10^{-9}$ [Fig. 1(b)]. An $f/2.5$ off-axis parabolic mirror was used to optimize the focal spot of the pump beam. The pump spot on the target (aluminum coated BK-7 glass) was ~ 40 μm [full width at half maximum (FWHM)], creating a peak intensity $I_L \sim 5 \times 10^{18}$ W/cm^2. The angle of incidence of the pump beam on the target was $\sim 45^\circ$. The cryogenic-cooled final amplifier of the laser system ensures a reasonably smooth spatial profile for the pump beam, mitigating unwanted transverse variations in the excitation. A small fraction of the main laser beam was redirected using a thin beam splitter and up-converted to its second harmonic (400 nm) by a β-barium borate (BBO) crystal. This up-converted beam was used as the probe pulse (duration $\sim$ 150 fs) for the experiment. The narrow bandwidth ($\sim$1.5 nm) of the second harmonic spectrum [Fig. 1(c)] facilitates the observation of small changes in the wavelength, as shown later. After passing through a high-resolution delay stage the probe was focused (FWHM $\sim$ 80 μm) on the pump-generated plasma at near normal incidence. Time matching between the pump and the probe was confirmed by monitoring probe reflectivity as a function of the time delay between the pump and the probe. The interaction point was imaged with an optical resolution of ~ 4 μm and a magnification of $\sim 90\times$. The reflected probe was collected by a lens and sent to the high-resolution (0.3-Å) multichannel spectrometer. The high-resolution multichannel spectrometer was designed with 16 fiber-equipped identical spectrometers [34]. All 16 spectra were recorded for each laser shot and spectra for each delay were collected over many dozens of shots.

Figure 2(a) shows three normalized reflected probe spectra measured at three different locations across the probe for 4.3 ps time delay. It shows different amounts of redshifts and

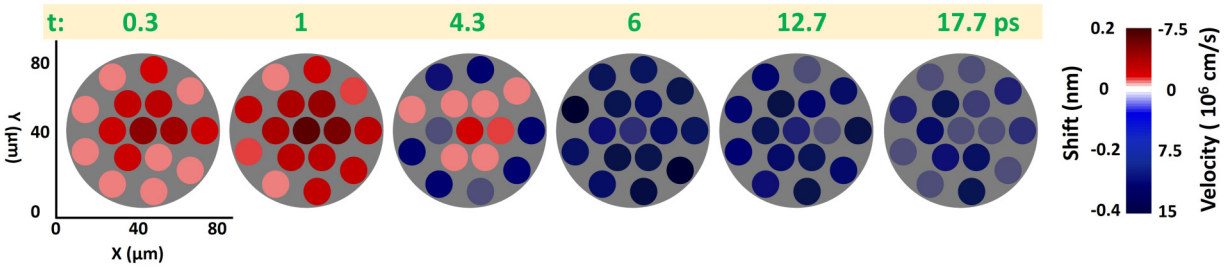

FIG. 3. Measured spatially resolved Doppler shifts and velocity maps for different time delays. Velocity maps are derived from measured Doppler shift data.

blueshifts at different locations. In order to infer the small-wavelength shifts more accurately, the normalized reference spectrum is subtracted from all the time-delayed reflected spectra (which are also normalized) and each curve is referred to as a difference amplitude curve [some such are shown in Fig. 2(b)]. For a blueshift, the difference amplitude changes its sign from positive to negative and vice versa for a redshift. Doppler shifts were calculated by subtracting the central wavelength of the reference spectrum (incident probe spectrum) from that of the reflected probe spectra. Doppler shifts measured at different locations across the probe beam for four different time delays are plotted in Fig. 2(c). Two-dimensional maps of the measured Doppler shifts at different time delays are presented in Fig. 3. Initially we observe a redshift from all positions and almost all are peaking at ∼1 ps. The central part of the probe shows a maximum redshift of ∼0.2 nm. After reaching a maximum, the redshift decreases with time and the sign of the shift changes to blue. Different transverse locations take different amounts of time to move from the redshift to blueshift. It is observed that the regions showing more redshift take more time to change the sign of the shift. The spatially resolved velocity (Fig. 3) was calculated using the relation [35] $V_{cr} = -0.5c\Delta\lambda/\lambda$, where λ is the incident probe wavelength, $\Delta\lambda$ is the Doppler shift, and c is the light speed in vacuum. Here, negative (redshift) and positive (blueshift) velocities indicate the inward and outward motion of the probe-critical density surface, respectively. The central part of the probed plasma layer shows a maximum inward velocity $\sim 7 \times 10^6$ cm/s at ∼1 ps. At ∼6 ps, the outer parts of the plasma show a maximum outward velocity $\sim 15 \times 10^6$ cm/s. From the time-dependent velocity data an acceleration map of the probe-density surface is also derived. The acceleration is found to be of the order of $\sim 10^{18}$ cm/s^2.

Physically interpreting the results of the experiment requires that the interaction be modeled using detailed numerical simulation codes. Simulating the hydrodynamics induced by the interaction of a high-intensity laser pulse with a solid target requires the use of several codes in a series. Here, the interaction between the initially solid target and the laser prepulse is first simulated using h2d, a 2D Lagrangian radiation hydrodynamics simulation code. [36] The output from this simulation is then employed to initialize a 2D particle-in-cell (PIC) code simulation using the EPOCH code [37]. Finally, the output from EPOCH is used to initialize a second h2d simulation which models the subsequent hydrodynamic evolution of the target. A time sequence of the results is shown in Fig. 4. As in previous work [10,11] the early time redshifting is seen to be a result of the pressure pulse launched in the plasma by the pump pulse, as it passes rapidly through the location of the probe's critical surface. The later time behavior corresponds to the plasma in that region settling into a stable rarefaction wave. Here, we also see that the timing of the transition between these two phases of behavior is a function of the location relative to the center of the pump-laser spot. The simulations agree well with the experimental results, particularly in terms of predicting a similar magnitude for the early time motion into the target and the timing of the transition from the redshift to blueshift in the center of the focal spot. Note that the exact agreement at the very earliest times may not be possible as not all physical parameters are parsed between the PIC and radiation hydrodynamics setups, as pointed out in our earlier works [10,11,14,16]. It proves to be quite challenging to model this problem due to the extreme sensitivity of the results to the interpolation method used in remapping the density profile in the transition between the EPOCH and h2d code. Submicron scale shifts in the position of the density contour of the probe can introduce a significant error in the predictions of the Doppler shift. The difficulty is compounded by the transition from a PIC framework dealing with particle number densities to a radiation hydrodynamics code that takes mass densities as its input. The fibers can be arranged in any geometry (line, cross, axisymmetric) in order

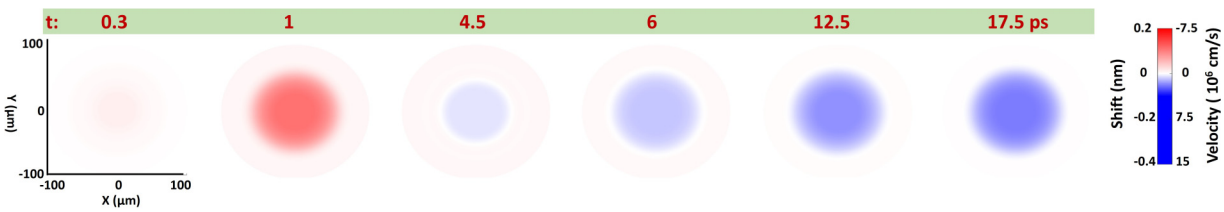

FIG. 4. A time sequence of simulation results generated using a combination of the h2d radiation-hydrodynamic and EPOCH PIC codes.

to most effectively capture the transverse velocity profile. However, in the present experiment the fibers were arranged in the manner described on the assumption that the behavior may not be axisymmetric. As the presence of filamentation instabilities and other effects can make the plasma dynamics highly nonuniform therefore, clearly the presence of 3D behavior is possible even where the target and/or laser geometry exhibit greater symmetry. In the 2D radiation hydrodynamics (rad-hydro) simulation, the results are axisymmetric, but that is a limitation of the 2D *r*-*z* simulation geometry. The plasma will become increasingly nonplanar as it evolves. However, the dense plasma remains relatively planar on the timescale of the experiment, and this is confirmed by the modeling.

Let us now compare our study with some others that monitor plasma evolution. Chirped pulse reflectometry and interferometry have so far been limited to one dimension and while they have been essential and successful in experiments with large lasers, the control and monitoring of chirp are important for deriving the time information [38]. It is also difficult, particularly in very-high-intensity laser-matter interactions or over long timescales, to unambiguously determine the effect of surface motion using frequency domain interferometry. Extension of this method to derive 2D spatial information simultaneously with temporal tracking appears quite complicated as it will need multiple interferometers to generate pairs of twin probe pulses as well as multiple spectrographs for different spatial points. In addition, the inference of spatial changes in each of them will need considerable data reduction. In an interesting study Evans *et al.* [39] did get some transverse information along the probe diameter at 10^{14} W/cm^2, using single color frequency domain interferometry. Their inference of the plasma evolution, however, was due to multiple factors such as "changes in the optical properties of the reflecting surface, motion of the reflecting surface, and change in the refractive index of the material between the reflecting surface and the observer." In contrast, in our experimental geometry we can isolate the effect of the velocity. The most popular technique for studying surface motion in laser-induced shocks is the velocity interferometer system for any reflector (VISAR) [40,41], where the time resolution is limited by the detectors used, typically a nanosecond to tens of a picosecond. Most of these studies were at modest intensities, a factor of 10^3–10^6 lower than those used here. Shadowgraphy [42] may give adequate time resolution but the spatial information is rather limited—the motion of the edge can be measured at some level in overdense plasmas, but difficult to resolve internal features. Sequentially timed all optical mapping photography (STAMP) [43] can give time information but the spatial data are restricted to one axis; this is also a very complex technique involving time and spatial mapping devices and microelectromechanical optical assemblies and sophisticated data reduction procedures. Shadowgraphy and STAMP are difficult to use for all target geometries (example: concave targets) and for oblique laser incidence. In comparison, the multipoint 2D Doppler spectrometry discussed in this paper is simpler, and works for oblique incidence and different target geometries, *simultaneously* in time and space for every laser shot and with chirped probe pulses, well suited to the petawatt and superpetawatt lasers that offer limited shots for each experiment. The present study is aimed at demonstrating the principle and the capabilities of the method. With better imaging, many spectrometers, and shorter or temporally shaped pulses, the spatial and temporal information can be greatly enhanced.

In conclusion, we presented the ultrafast time-resolved and two-dimensional spatially resolved evolution of the motion of a plasma created by the interaction of an ultrahigh-intensity laser with a solid target, using two-dimensional Doppler velocimetry. In combination with 2D PIC and 2D radiation hydrodynamics simulations the femtosecond-resolved velocity maps reveal interesting features such as the inward motion of the plasma driven by the pump pulse, the extent and duration of which is a function of the position relative to the center of the pump laser focal spot. The diagnostic technique itself has the potential to provide as yet unavailable detail in its rendering of the complex dynamics of short-pulse laser-plasma interactions at high intensities, enabling temporal resolutions of less than 100 fs and a transverse spatial resolution of only a few microns. Such velocity (temperature) maps may provide crucial information on the evolution of lateral energy transport, particularly under ultrashort-pulse excitation, and may provide valuable insights into the physics of the interaction.

G.R.K. acknowledges support via J. C. Bose Fellowship Grant No. JCB-037/2010 from the Science and Engineering Research Board, Government of India. The authors thank B. Om Subham, Chandra V. Kotyada, and V. Rakesh Kumar for their help in the experiment.

[1] R. P. Drake, *High Energy Density Physics* (Springer, Berlin, 2006).

[2] P. Gibbon, *Short Pulse Laser Interactions With Matter* (Imperial College Press, London, 2005).

[3] P. K. Kaw, Nonlinear laser-plasma interactions, Rev. Mod. Plasma Phys. **1**, 2 (2017).

[4] Y. T. Li, C. Li, M. L. Zhou, W. M. Wang, F. Du, W. J. Ding, X. X. Lin, F. Liu, Z. M. Sheng, X. Y. Peng, L. M. Chen, J. L. Ma, X. Lu, Z. H. Wang, Z. Y. Wei, and J. Zhang, Strong terahertz radiation from relativistic laser interaction with solid density plasmas, Appl. Phys. Lett. **100**, 254101 (2012).

[5] S. Cipiccia, M. R. Islam, B. Ersfeld, R. P. Shanks, E. Brunetti, G. Vieux, X. Yang, R. C. Issac, S. M. Wiggins, G. H. Welsh, M.-P. Anania, D. Maneuski, R. Montgomery, G. Smith, M. Hoek, D. J. Hamilton, N. R. C. Lemos, D. Symes, P. P. Rajeev, V. O. Shea *et al.*, Gamma-rays from harmonically resonant betatron oscillations in a plasma wake, Nat. Phys. **7**, 867 (2011).

[6] J. Faure, Y. Glinec, A. Pukhov, S. Kiselev, S. Gordienko, E. Lefebvre, J. P. Rousseau, F. Burgy, and V. Malka, A laser-plasma accelerator producing monoenergetic electron beams, Nature (London) **431**, 541 (2004).

[7] H. Chen, S. C. Wilks, J. D. Bonlie, E. P. Liang, J. Myatt, D. F. Price, D. D. Meyerhofer, and P. Beiersdorfer, Relativistic Positron Creation Using Ultraintense Short Pulse Lasers, Phys. Rev. Lett. **102**, 105001 (2009).

[8] L. Robson, P. T. Simpson, R. J. Clarke, K. W. D. Ledingham, F. Lindau, O. Lundh, T. McCanny, P. Mora, D. Neely, C.-G. Wahlstrom, M. Zepf, and P. McKenna, Scaling of proton acceleration driven by petawatt-laser-plasma interactions, Nat. Phys. **3**, 58 (2007).

[9] R. Rajeev, T. M. Trivikram, K. P. M. Rishad, V. Narayanan, E. Krishnakumar, and M. Krishnamurthy, A compact laser-driven plasma accelerator for megaelectronvolt-energy neutral atoms, Nat. Phys. **9**, 185 (2013).

[10] S. Mondal, A. D. Lad, S. Ahmed, V. Narayanan, J. Pasley, P. P. Rajeev, A. P. L. Robinson, and G. R. Kumar, Doppler Spectrometry for Ultrafast Temporal Mapping of Density Dynamics in Laser-Induced Plasmas, Phys. Rev. Lett. **105**, 105002 (2010).

[11] A. Adak, D. R. Blackman, G. Chatterjee, P. K. Singh, A. D. Lad, P. Brijesh, A. P. L. Robinson, J. Pasley, and G. R. Kumar, Ultrafast dynamics of a near-solid-density layer in an intense femtosecond laser-excited plasma, Phys. Plasma **21**, 062704 (2014).

[12] K. Jana, A. D. Lad, M. Shaikh, V. R. Kumar, D. Sarkar, Y. M. Ved, J. Pasley, A. P. L. Robinson, and G. R. Kumar, Generation of a strong reverse shock wave in the interaction of a high-contrast high-intensity femtosecond laser pulse with a silicon target, Appl. Phys. Lett. **114**, 254103 (2019).

[13] M. Shaikh, K. Jana, A. D. Lad, I. Dey, S. L. Roy, D. Sarkar, Y. M. Ved, A. P. L. Robinson, J. Pasley, and G. R. Kumar, Tracking ultrafast dynamics of intense shock generation and breakout at target rear, Phys. Plasma **25**, 113106 (2018).

[14] A. Adak, P. K. Singh, D. R. Blackman, A. D. Lad, G. Chatterjee, J. Pasley, A. P. L. Robinson, and G. R. Kumar, Controlling femtosecond-laser-driven shock-waves in hot, dense plasma, Phys. Plasma **24**, 072702 (2017).

[15] Y. Ping, A. J. Kemp, L. Divol, M. H. Key, P. K. Patel, K. U. Akli, F. N. Beg, S. Chawla, C. D. Chen, R. R. Freeman, D. Hey, D. P. Higginson, L. C. Jarrott, G. E. Kemp, A. Link, H. S. McLean, H. Sawada, R. B. Stephens, D. Turnbull, B. Westover *et al.*, Dynamics of Relativistic Laser-Plasma Interaction on Solid Targets, Phys. Rev. Lett. **109**, 145006 (2012).

[16] A. Adak, A. P. L. Robinson, P. K. Singh, G. Chatterjee, A. D. Lad, J. Pasley, and G. R. Kumar, Terahertz Acoustics in Hot Dense Laser Plasmas, Phys. Rev. Lett. **114**, 115001 (2015).

[17] K. Jana, D. R. Blackman, M. Shaikh, A. D. Lad, D. Sarkar, I. Dey, A. P. L. Robinson, J. Pasley, and G. R. Kumar, Probing ultrafast dynamics of solid-density plasma generated by high-contrast intense laser pulses, Phys. Plasma **25**, 013102 (2018).

[18] J. Metzkes, K. Zeil, S. D. Kraft, M. Rehwald, T. E. Cowan, and U. Schramm, Reflective optical probing of laser-driven plasmas at the rear surface of solid targets, Plasma Phys. Control. Fusion **58**, 034012 (2016).

[19] V. Bagnoud, J. Hornung, T. Schlegel, B. Zielbauer, C. Brabetz, M. Roth, P. Hilz, M. Haug, J. Schreiber, and F. Wagner, Studying the Dynamics of Relativistic Laser-Plasma Interaction on Thin Foils by Means of Fourier-Transform Spectral Interferometry, Phys. Rev. Lett. **118**, 255003 (2017).

[20] M. P. Kalashnikov, P. V. Nickles, Th. Schlegel, M. Schnuerer, F. Billhardt, I. Will, W. Sandner, and N. N. Demchenko, Dynamics of Laser-Plasma Interaction at 10^{18} W/cm^2, Phys. Rev. Lett. **73**, 260 (1994).

[21] R. A. Cairns, Resonant absorption at a rippled critical surface, Plasma Phys. **20**, 991 (1978).

[22] S. C. Wilks, W. L. Kruer, M. Tabak, and A. B. Langdon, Absorption of Ultra-Intense Laser Pulses, Phys. Rev. Lett. **69**, 1383 (1992).

[23] A. Macchi, F. Cornolti, F. Pegoraro, T. V. Liseikina, H. Ruhl, and V. A. Vshivkov, Surface Oscillations in Overdense Plasmas Irradiated by Ultrashort Laser Pulses, Phys. Rev. Lett. **87**, 205004 (2001).

[24] D. W. Schumacher, G. E. Kemp, A. Link, R. R. Freeman, and L. D. Van Woerkom, The shaped critical surface in high intensity laser plasma interactions, Phys. Plasmas **18**, 013102 (2011).

[25] B. T. Bowes, H. Langhoff, M. C. Downer, M. Wilcox, B. Hou, J. Nees, and G. Mourou, Femtosecond microscopy of radial energy transport in a micrometer-scale aluminum plasma excited at relativistic intensity, Opt. Lett. **31**, 116 (2006).

[26] H. Langhoff, B. T. Bowes, M. C. Downer, B. Hou, and J. A. Nees, Surface energy transport following relativistic laser-solid interaction, Phys. Plasmas **16**, 072702 (2009).

[27] P. K. Singh, Y. Q. Cui, G. Chatterjee, A. Adak, W. M. Wang, S. Ahmed, A. D. Lad, Z. M. Sheng, and G. R. Kumar, Direct observation of ultrafast surface transport of laser-driven fast electrons in a solid target, Phys. Plasma **20**, 110701 (2013).

[28] M. Borghesi, S. Bulanov, D. H. Campbell, R. J. Clarke, T. Zh. Esirkepov, M. Galimberti, L. A. Gizzi, A. J. MacKinnon, N. M. Naumova, F. Pegoraro, H. Ruhl, A. Schiavi, and O. Willi, Macroscopic Evidence of Soliton Formation in Multiterawatt Laser-Plasma Interaction, Phys. Rev. Lett. **88**, 135002 (2002).

[29] C. A. J. Palmer, J. Schreiber, S. R. Nagel, N. P. Dover, C. Bellei, F. N. Beg, S. Bott, R. J. Clarke, A. E. Dangor, S. M. Hassan, P. Hilz, D. Jung, S. Kneip, S. P. D. Mangles, K. L. Lancaster, A. Rehman, A. P. L. Robinson, C. Spindloe, J. Szerypo, M. Tatarakis *et al.*, Rayleigh-Taylor Instability of an Ultrathin Foil Accelerated by the Radiation Pressure of an Intense Laser, Phys. Rev. Lett. **108**, 225002 (2012).

[30] G. J. Rickard, A. R. Bell, and E. M. Epperlien, 2D Fokker-Planck Simulations of Short-Pulse Laser-Plasma Interactions, Phys. Rev. Lett. **62**, 2687 (1989).

[31] E. G. Gamaly, Instability of the overdense plasma boundary induced by the action of a powerful photon beam, Phys. Rev. E **48**, 2924 (1993).

[32] Y. Wan, I. Andriyash, W. Lu, W. B. Mori, and V. Malka, Effects of the Transverse Instability and Wave Breaking on the Laser-Driven Thin Foil Acceleration, Phys. Rev. Lett. **125**, 104801 (2020).

[33] F. Lindau, O. Lundh, A. Persson, P. McKenna, K. Osvay, D. Batani, and C. G. Wahlstrom, Laser-Accelerated Protons with Energy-Dependent Beam Direction, Phys. Rev. Lett. **95**, 175002 (2005).

[34] K. Jana, A. D. Lad, Y. M. Ved, A. P. L. Robinson, J. Pasley, and G. R. Kumar, Ultrafast time-resolved two-dimensional velocity mapping of the hot-dense plasmas generated by intense-laser pulses (unpublished).

[35] X. Liu and D. Umstadter, Competition between Ponderomotive and Thermal Forces in Short-Scale-Length Laser Plasmas, Phys. Rev. Lett. **69**, 1935 (1992).

[36] H2d is a commercial product of Cascade Applied Sciences, https://casinc.com/h2d.html, email: larsen@casinc.com.

[37] T. Arber, K. Bennett, C. S. Brady, A. Lawrence-Douglas, M. G. Ramsay, N. J. Sircombe, P. Gillies, R. G. Evans, H. Schmitz, A. R. Bell, and C. P. Ridgers, Contemporary particle-in-cell

approach to laser-plasma modelling, Plasma Phys. Controlled Fusion **57**, 113001 (2015).

[38] A. Benuzzi-Mounaix, M. Koenig, and J. M. Boudenne, Chirped pulse reflectivity and frequency domain interferometry in laser driven shock experiments, Phys. Rev. E **60**, R2488 (1999).

[39] R. Evans, A. D. Badger, F. Falliès, M. Mahdieh, T. A. Hall, P. Audebert, J. P. Geindre, J. C. Gauthier, A. Mysyrowicz, G. Grillon, and A. Antonetti, Time- and Space-Resolved Optical Probing of Femtosecond-Laser-Driven Shock Waves in Aluminum, Phys. Rev. Lett. **77**, 3359 (1996).

[40] L. M. Barker and R. E. Hollenbach, Laser interferometer for measuring high velocities of any reflecting surface, J. Appl. Phys. **43**, 4669 (1972).

[41] P. M. Celliers, D. K. Bradley, G. W. Collins, D. G. Hicks, T. R. Boehly, and W. J. Armstrong, Line-imaging velocimeter for shock diagnostics at the OMEGA laser facility, Rev. Sci. Instrum. **75**, 4916 (2004).

[42] N. Zhang, W. Wang, X. Zhu, J. Liu, K. Xu, P. Huang, J. Zhao, R. Li, and M. Wang, Investigation of ultrashort pulse laser ablation of solid targets by measuring the ablation-generated momentum using a torsion pendulum, Opt. Express **19**, 8870 (2011).

[43] K. Nakagawa, A. Iwasaki, Y. Oishi, R. Horisaki, A. Tsukamoto, A. Nakamura, K. Hirosawa, H. Liao, T. Ushida, K. Goda, F. Kannari, and I. Sakuma, Sequentially timed all-optical mapping photography (STAMP), Nat. Photonics **8**, 695 (2014).